ACCOUNTS
of chemical research

Photon-Based Techniques for Nondestructive Subsurface Analysis of Painted Cultural Heritage Artifacts

K. JANSSENS,*,† J. DIK,‡ M. COTTE,§ AND J. SUSINI§

†University of Antwerp, Antwerp, Belgium, ‡Delft University of Technology, Delft, The Netherlands, §European Synchrotron Radiation Facility, Grenoble, France

RECEIVED ON OCTOBER 24, 2009

CONSPECTUS

Often, just micrometers below a painting's surface lies a wealth of information, both with Old Masters such as Peter Paul Rubens and Rembrandt van Rijn and with more recent artists of great renown such as Vincent Van Gogh and James Ensor. Subsurface layers may include underdrawing, underpainting, and alterations, and in a growing number of cases conservators have discovered abandoned compositions on paintings, illustrating artists' practice of reusing a canvas or panel.

The standard methods for studying the inner structure of cultural heritage (CH) artifacts are infrared reflectography and X-ray radiography, techniques that are optionally complemented with the microscopic analysis of cross-sectioned samples. These methods have limitations, but recently, a number of fundamentally new approaches for fully imaging the buildup of hidden paint layers and other complex three-dimensional (3D) substructures have been put into practice. In this Account, we discuss these developments and their recent practical application with CH artifacts. We begin with a tabular summary of 14 IR- and X-ray-based imaging methods and then continue with a discussion of each technique, illustrating CH applications with specific case studies.

X-ray-based tomographic and laminographic techniques can be used to generate 3D renditions of artifacts of varying dimensions. These methods are proving invaluable for exploring inner structures, identifying the conservation state, and postulating the original manufacturing technology of metallic and other sculptures. In the analysis of paint layers, terahertz time-domain spectroscopy (THz-TDS) can highlight interfaces between layers in a stratigraphic buildup, whereas macrosopic scanning X-ray fluorescence (MA-XRF) has been employed to measure the distribution of pigments within these layers. This combination of innovative methods provides topographic and color information about the micrometer depth scale, allowing us to look "into" paintings in an entirely new manner.

Over the past five years, several new variants of traditional IR- and X-ray-based imaging methods have been implemented by conservators and museums, and the first reports have begun to emerge in the primary research literature. Applying these state-of-the-art techniques in a complementary fashion affords a more comprehensive view of paintings and other artworks.

1. Introduction

Below the surface of paintings by Old Masters such as Rubens and Rembrandt but also by more recent artists of great renown such as Van Gogh and Ensor, often a wealth of information is present, e.g., in the form of underdrawings, underpaintings, and alterations.[1] Many conservators have discovered abandoned compositions on paintings, illustrating the artists' practice to reuse

Published on the Web 05/12/2010 www.pubs.acs.org/acr
10.1021/ar900248e

TABLE 1. Overview of Imaging Methods Suitable for Nondestructive Subsurface Examination of Paintings and Related Works of Art

imaging method	acronym	contrast type	information imaged	dimensionality	resolution (μm)	photon source	refs
(A) X-ray-Based Methods							
(A1) Full-Field Imaging Methods							
macroscopic X-ray radiography	XRR	absorption	(electron) density	2D	>500	X-ray tube/SR	4
macroscopic computed tomography	CT	absorption	(electron) density	3D	>600	X-ray tube	5−7
microscopic computed tomography	MCT, μ-CT	absorption	(electron) density	3D	0.3−10	X-ray tube/SR	8−10
phase contrast tomography		refraction	interfaces	3D	0.3−10	SR	10, 13−15, 18, 19
laminography		absorption	(electron) density	3D	>1	SR	18−20
(A2) Scanned Beam Methods							
microscopic XRF mapping	μ-XRF	elemental	elemental composition	2D	>0.1[b]	X-ray tube/SR	21−23
microscopic XANES mapping	μ-XANES	chemical state	species composition	2D	>0.1[b]	SR	22, 23
microscopic XRD mapping	μ-XRD	crystal structure	phase composition	2D	>0.1[b]	X-ray tube/SR	12, 21, 23
macroscopic scanning XRF	MA-XRF	elemental	elemental composition	2D	250−1000	X-ray tube/SR	30−32
confocal micro-XRF	CXRF	elemental	elemental composition	3D[a]	>10[c]	X-ray tube/SR	26−29
micro-XRF/XRD tomography		elemental/crystal strusture	element/phase composition	3D[a]	>0.3[b]	SR	12
(B) Infrared Tetrahertz Radiation-Based Methods							
infrared reflectography	IRR	absorption	absorbing species	2D	>1000	IR lamp	34
optical coherence tomography	OCT	absorption	absorbing species	3D	>1000, >1[d]	IR lamp	35−37
tetrahertz time-domain spectroscopic imaging	THz-TDS	optical density	interfaces	3D[a]	>1000, >20[d]	THz laser	38

[a] Usually only selected planes in the examined volume imaged. [b] Depends on the primary beam size. [c] Depends on the fluorescent energy, typically 10−40 μm. [d] Estimated depth resolution.

a canvas or panel.[2] Many painterly effects critically depend on the layer buildup; e.g., the translucent shine of colorful tissues, the suggestion of shadow in fleshtones, or the illusion of an object's texture may be realized by deliberately including the optical contribution of lower layers. Knowledge about the stratigraphy of a painting often is highly relevant in conservation when stability problems such as paint discoloration or delamination are considered. Thus, the study of a painting's stratigraphy is a research theme common to curators, conservators, and conservation scientists.

Traditionally, the visualization of the inner structure of painted cultural heritage (CH) artifacts relies on penetrative, two-dimensional imaging techniques such as infrared reflectography (IRR) and X-ray radiography (XRR), optionally complemented with microscopic analysis of cross-sectioned samples.[3] However, there are significant limitations to this approach.

(a) The imaging techniques are sensitive to a limited number of materials and provide only flat, two-dimensional (2D) images of complex, three-dimensional (3D) structured systems. (b) Cross sections require destructive sampling that (c) provides only local information.

Recently, a number of new approaches of imaging the integral, three-dimensional buildup of hidden paint layers systems were proposed and put into practice. They can be considered to be modernized extensions of IRR and XRR.

Terahertz time-domain spectroscopy (THz-TDS) can be used to map interfaces inside a paint multilayer. Laminography, a variant of X-ray absorption tomography, is a method that allows visualization in three dimensions of the density variations inside a small subvolume a much larger painting. Macroscopic scanning X-ray fluorescence (MA-XRF) has been employed to visualize the distribution of pigments within some of these layers. Combined use of these methods provides topographic and color information about the micrometer depth scale, essential parameters for looking "into" paintings on an entirely new level.

After outlining their principles (see Table 1), we discuss the first CH cases studied with these new methods, highlighting their possibilities of extracting information about the inner structure of painted artworks.

2. X-ray-Based Methods

Because X-rays can penetrate almost any object and yield information about the interior of specimens opaque to visible light, since their discovery they have been used as a powerful tool for nondestructive inspection of materials. While the art and museum world heavily relies on XRR for the visualization of the invisible inner structure of paintings, conven-

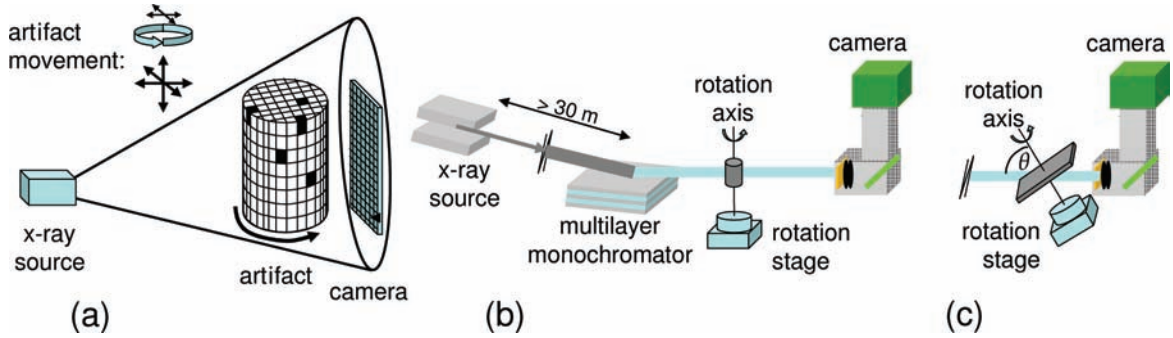

FIGURE 1. Principle of different variants of X-ray absorption-computed tomography: (a) fan-beam tomography (X-ray tube source), (b) parallel beam tomography (synchrotron source), and (c) laminography.

tional (X-ray tube-based) XRR[4] has a number of important limitations. Since the observed X-ray absorbance is a summation of all element-specific absorbances, the contributions to the overall image contrast from (small quantities of) weakly absorbing elements will frequently be obscured by those of heavier elements that are present in higher concentrations. Thus, the absorption contrast in XRR images is mostly caused by the heavy metal paint components (e.g., lead in lead white, mercury in vermillion). Moreover, since canvases usually are primed with a homogeneous lead white layer, an overall absorbance background is often present. Finally, the polychromatic character of an X-ray tube also reduces the contrast. Thus, conventional XRR images of paintings frequently provide only a fragmentary view of their substructure, hampering the readability of hidden compositions.

2.1. Tomographic Imaging. 2.1.1. Principle. The images produced by XRR may also be blurred because the entire 3D shape of the irradiated object becomes projected onto a 2D screen or camera. To circumvent this, X-ray tomography makes use of an extended series of projection images recorded under many different angles between the object and primary beam; the object hereby rotates around an axis perpendicular to the source−detector axis (Figure 1a). Mathematical reconstruction then allows creation of a virtual, 3D rendition of the object's shape and (inner) density variations and visualization of its inner parts without physically sectioning or otherwise destroying it. This can be done both at the macroscopic (decimeter to meter) level, e.g., in medical computed tomography (CT), and at the microscopic level (MCT).

2.1.2. Macro-CT and Micro-CT. Macro-CT has been widely used for 3D visualization, for both medical and nonmedical purposes.[5] There are far less stringent limitations with regard to X-ray exposure and scanning time for the examination of CH artifacts in wood, paper, glass, or metals instead of patients. A recent report describes the X-ray CT inspection of the sculpture of the Egyptian pharaoh-queen Nefertiti (18th dynasty), one of the treasures of ancient Egyptian art,[6] with the aim of assessing its conservation status and of gaining information about its creation. Multisection CT with a section thickness of 0.6 mm was performed, resulting in the observation that the stucco layer on the face and the ears was very thin (1−2 mm) while the rear part of the reconstructed crown showed two thick stucco layers of different attenuation values, indicating the use of a multistep manufacturing process. The discovery of air voids in the stucco and of filamentous fissures parallel to the surface led to the conclusion that very careful handling of this artifact is mandatory to avoid any pressure and shearing forces in the crown and the shoulders. Another example involved the study of Roman glass fragments contained within large clumps of soil, excavated from a burial site.[7] High-resolution tomography allowed "virtual removal" of the soil, making it possible to determine the shape and morphological class of five of the 14 excavated objects. In addition, CT was useful for the reconstruction of the layout of the burial chamber, the compilation of a list of grave contents, and the positioning of these contents within the chamber.

Next to medical style macro-CT equipment, several manufacturers offer table top MCT instruments with an effective spatial resolution typically situated in the 1−10 μm range; "nanotomographic" equipment (resolution between 0.2 and 1 μm) is also available. MCT has been successfully applied in many fields such as archeology, soil science, and biology. Bugani et al. recently used MCT for quantitatively estimating the changes in the porosity of sandstone[8] and of archeological waterlogged wood[9] after consolidation treatments.

2.1.3. Full-Field 3D Imaging by Means of Synchrotron Radiation (SR). The improving availability and performance of synchrotron radiation sources has significantly boosted the 3D imaging possibilities of paintings and paint layer stacks. Synchrotrons are large particle accelerators that produce intense, quasi-parallel beams of X-rays, at flux levels many orders of magnitude higher than those of X-ray tubes. Monochromatic beams of tunable energy with very small cross sec-

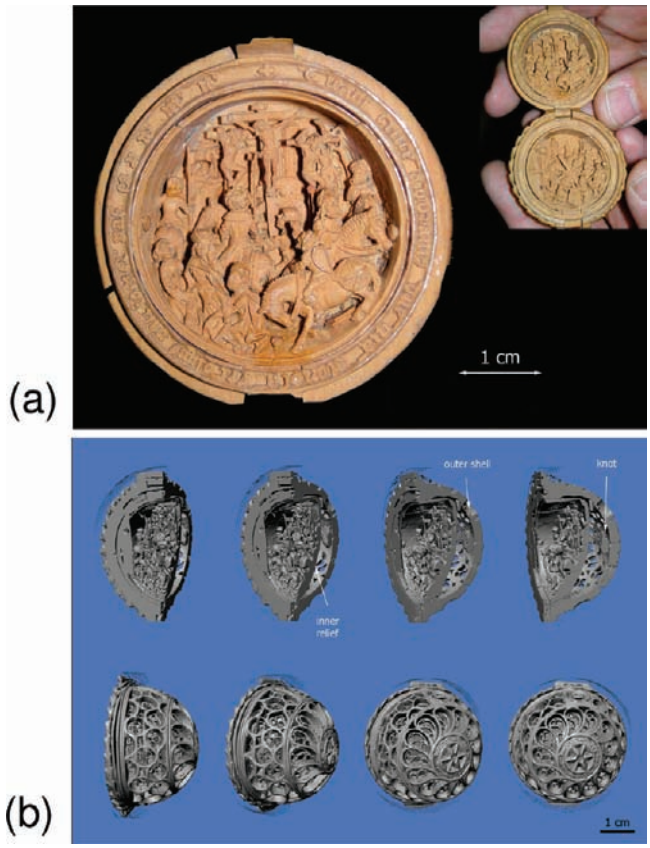

FIGURE 2. (a) Photograph of a 16th Century prayer nut and (b) (top row) volume reconstructions with a vertical cut through the middle of the nut, revealing the shell structure, and (bottom row) volume reconstructions of the outer shell with a Gothic motif.

tions (in the micrometer to tens of nanometers range)[10] can be generated. The results of CT investigation of an early 16th Century prayer nut,[11] a spherical wooden object ca. 4 cm in diameter, are shown in Figure 2; its interior holds highly finished miniature wood carvings with scenes from the life of Christ with carving details well beyond the millimeter scale. CT revealed that the central part of the relief was cut from a single piece of wood, rather than assembled from multiple components, underlining the extraordinary manual dexterity of its maker.

Next to making use of absorption contrast, where a transmission detector records the amount of radiation that disappears inside the irradiated object, other types of CT, based on fluorescence, diffraction/scattering,[12] and refraction[13] of X-rays, were developed. Phase-contrast CT exploits enhanced edge contrast caused by interference between the original X-ray beam and its refracted equivalent. In slightly absorbing materials, this significantly improves the clarity with which the interfaces between various material phases may be visualized. Via measurement of the thickness of the growth layers inside teeth of key Neanderthal fossils, information about

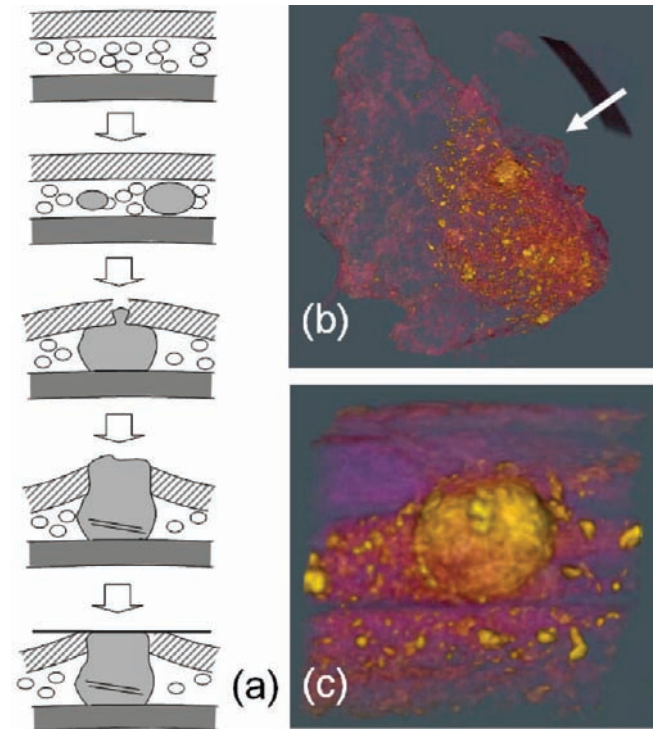

FIGURE 3. Visualization of a spherical lead soap protrusion by high-resolution absorption tomography (ESRF-ID19): (a) mechanism of protrusion formation and (b and c) views of a large protrusion (ca. 100 μm in diameter).

the age, food habits, and health of these prehistoric men could be revealed.[14] Also extinct insects, trapped in opaque amber, could be visualized in this manner.[15]

MCT (Figure 1b) is also a very promising technique for the inspection of stratigraphic paint layer samples without the need of physically embedding them into a resin and cross-sectioning them, a procedure after which only the exposed surface is available for microscopic inspection and analysis. Already embedded paint fragments can also be studied. The possibilities of MCT for obtaining virtual cross sections of small, submillimeter-sized, paint layer samples with the traditional, semidestructive embedding and polishing method were recently compared, leading to the conclusion that nearly equivalent information can be obtained.[16] Figure 3 shows 3D renditions of a spherical lead-soap protrusion that formed below the surface of a 15th Century painting as a result of the saponification reaction of Pb^{2+} ions (from lead white) with fatty acid residues in oil paint; their gradual increase in size can lead to the puncture of the originally closed paint surface.[17] MCT allows observation of the in situ growth of such bodies, e.g., during accelerated aging treatments.

2.1.4. Laminography. The types of tomography mentioned above require that the lateral dimensions of artifacts being examined are all roughly the same so that under all

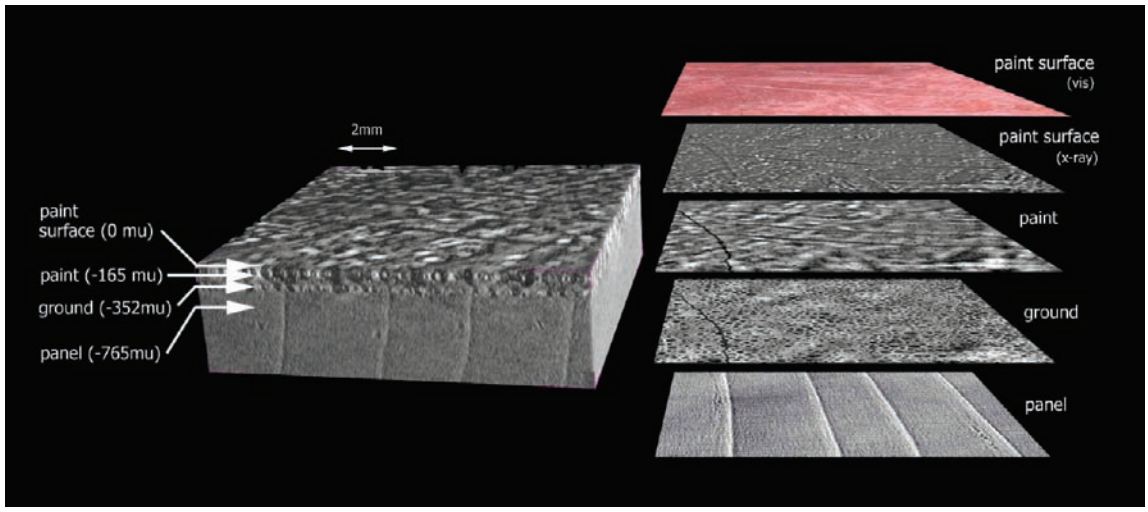

FIGURE 4. Laminographic images obtained a various depths below the surface of a test painting. The texture of the various layers can be inspected in detail.

observation and irradiation angles, the total path length through the material that the transmitted radiation must follow does not vary more than, say, one order of magnitude. In case of paintings and other objects that are much more extended along two dimensions (length and width) than along the third (depth), conventional CT cannot be employed; during the rotation of the painting relative to the source−detector axis, in a particular orientation, its entire length or width would be in the radiation path, blocking all transmission. The related method of laminography, originally developed for the inspection of complex, flat, multilayered objects such as printed circuit boards,[18] does not suffer this limitation; the rotation takes place around an axis that is tilted relative to the radiation source−detector axis (Figure 1c).

Experiments on mock-up paintings[19] showed that voids and hidden compartments can be visualized in a nondestructive manner via this technique as well as the texture of the different layers in a stratigraphy[20] (Figure 4).

2.2. Scanned Beam Imaging. While the full-field forms of tomography are excellent for 3D imaging of density variations or of interfaces between materials, they are not sensitive to changes in elemental makeup, speciation, or crystallographic composition. Imaging by means of a scanning X-ray micro- or nanobeam while various material-specific signals are recorded can provide more detailed information of this type. Both monochromatic and polychromatic beams can be used, and in some cases, the energy of the monochromatic beams is varied, allowing for spectroscopic imaging. Often the total amount of transmitted, reflected, and/or scattered photons is recorded while energy-dispersive photon detectors are frequently employed.

According to Bertrand et al.,[21] in the period from 1986 to 2005, the most important (scanning) method of investigation was XRF (yielding information about the local elemental composition), followed by X-ray diffraction (XRD) (local crystallographic phases), X-ray absorption spectroscopy (XAS) (chemical state/electronic environment contrast), and Fourier-transform infrared (FTIR) spectroscopy (presence and distribution of specific types of molecules and/or chemical bonds). Cotte et al.[22] have reviewed the use of (combinations) of these methods for the investigation of various types of cultural heritage materials, among which are (partially) altered paint layer stratigraphies. The distribution of Cd compounds at or just below the surface of altered cadmium yellow (CdS) samples derived from a painting of the avant-garde painter James Ensor (1860−1949)[23] was studied in this manner. As demonstrated by μ-XRD and μ-XANES (X-ray absorption near-edge spectroscopy), the alteration involved the oxidation of CdS to $CdSO_4 \cdot 2H_2O$ under the influence of light, oxygen, and moisture (Figure 5). Sulfur species-specific imaging versus depth showed that during the last century, the sulfur oxidation front progressed ca. 10 μm below the surface. These observations are relevant for painting conservators when they are establishing optimal conditions (relative humidity and level and type of illumination) for long-term preservation of works of art.

2.3. Micro- and Macro-XRF. In case energetic primary radiation is employed to induce the emission of characteristic radiation, XRF signals not only are generated superficially but also emerge from extended depths (several tens to hundreds of micrometers) below the surface of the material. This phenomenon was exploited in two different manners for oil painting imaging (Figure 6): either by employing confocal μ-XRF, a depth-selective variant of μ-XRF, or by employing

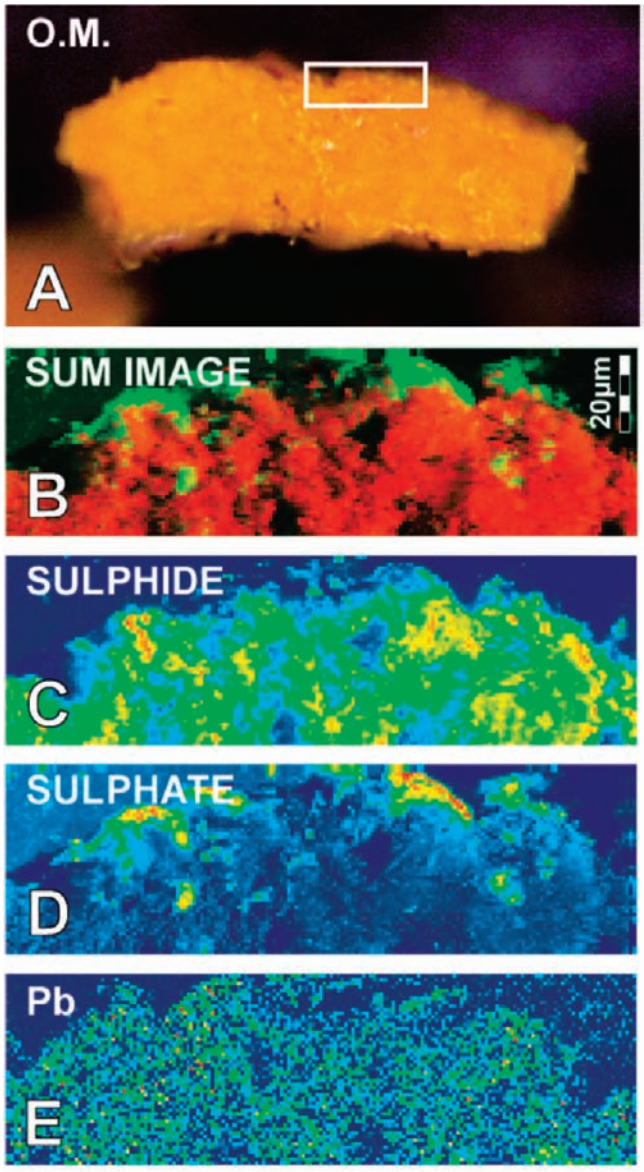

FIGURE 5. (A) Optical micrograph of a cross section of the partially degraded paint surface. (B) RG composite S chemical state map of panels C and D (red for sulfides and green for sulfates). Distribution maps of (C) sulfides (2.4730 keV) and (D) sulfates (2.4820 keV). Map size of 184 μm $\times$ 50 μm; step size of 1 μm $\times$ 1 μm. (E) Pb distribution. Reprinted with permission from ref 23. Copyright 2009 American Chemical Society.

highly energetic millibeams of primary X-rays that are scanned over large areas of a painting (MA-XRF).

2.3.1. Confocal μ-XRF. Scanning electron microscopy supplemented with energy-dispersive X-ray spectroscopy (SEM-EDS)[24] is often employed for paint layer characterization. While powerful, this technique requires a sample to be extracted from the painting. Typically, only a limited number of samples may be taken, especially from the areas of greatest interest, such as the facial area in a portrait. During the past several years, improvements to X-ray optics based on

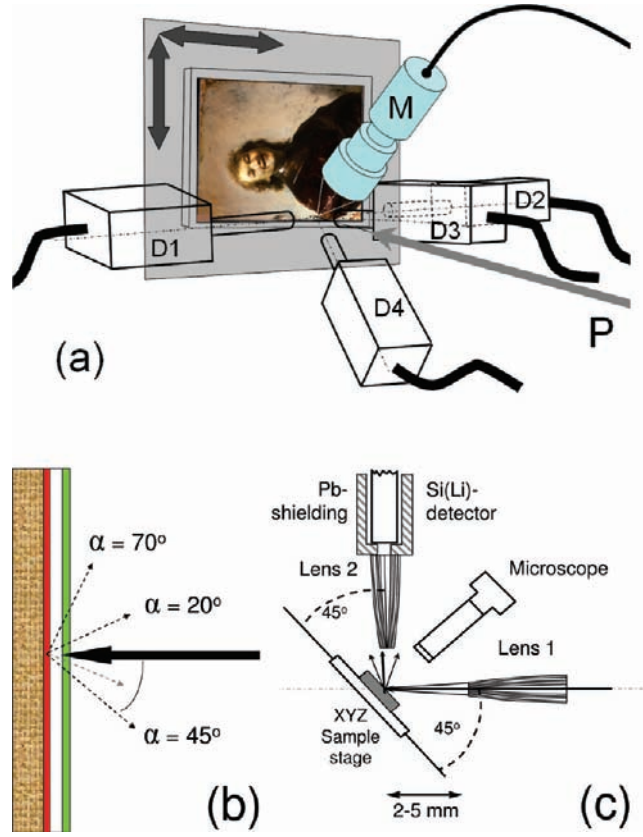

FIGURE 6. Irradiation−detection geometry (a) of MA-XRF using multiple detectors D1−-D4 (M denotes the video camera/microscope and P the primary beam). (b) Top view, showing different takeoff angles (α) associated with different detectors (c) of confocal XRF.

hollow glass capillary tubes have led to the development of depth selective or confocal μ-XRF (CXRF)[25] employing two X-ray lenses with coinciding foci (Figure 6c). One optic focuses the incident beam, while the other, perpendicular to the first, gathers X-ray fluorescence only from the microregion of the sample where the focal cone of the second optic intersects that of the first. By scanning materials through this volume, one can obtain intensity profiles reflecting the local composition variation versus depth or versus a lateral coordinate with a resolution in the range of 10−50 μm. While for primary beam focusing, several types of X-ray lenses may be used, as collecting optics for the fluorescent radiation, only polycapillary lenses,[26] consisting of a tapered bundle of many thousands of hollow glass tubes, are employed.

A promising feature of CXRF is the possibility of providing information not only about the 3D distribution of different elements in a sample but also about their local concentrations. To do so, one must first determine the elemental composition of the outermost layers in a multilayered material and then calculate the effect of absorption by those layers on the fluorescence intensity from layers buried below.[27,28] When the

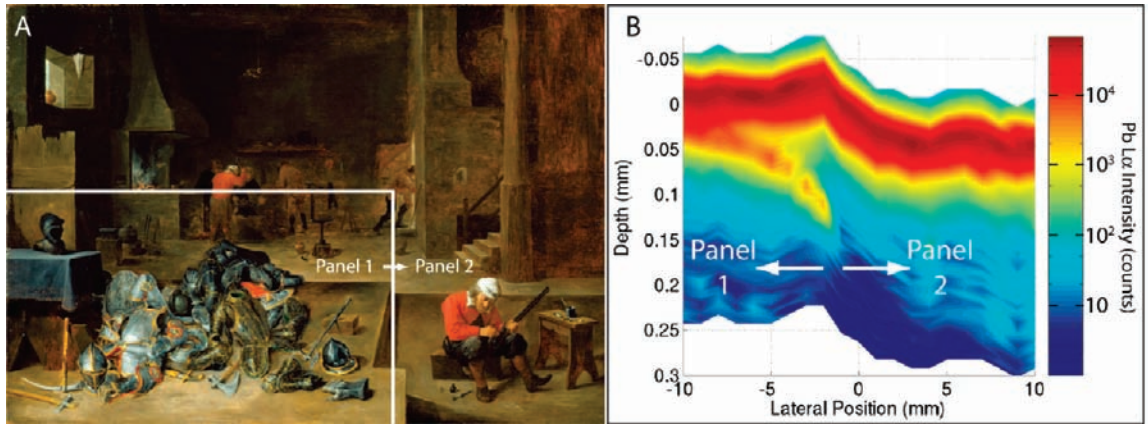

FIGURE 7. (A) Teniers' 'Armourers Workshop' and (B) in-depth distribution of Pb, as obtained by CXRF, revealing the discontinuity between panel 1 and panel 2 in the paint layers at a depth of ca. 100 μm below the surface.

energy-dependent resolution of the confocal microscope is explicitly taken into account, the position and thickness of buried layers can be more precisely determined than the nominal, instrumental resolution. Woll et al.[29] have employed CXRF to examine the continuity of the paint layers across a joint between two panels present in Breugel's 'The Armorers Shop'. The resulting depth distribution of Pb (Figure 7B) clearly shows that only the upper paint layers are continuous and that the original paint layers were applied separately on both panels, prior to their merger.

2.3.2. High-Energy MA-XRF. Upon irradiation with an energetic X-ray beam (see Figure 6a,b), the covering surface layers will not significantly attenuate the high-energy fluorescence signals from heavy elements in the deeper layers; in this manner, the distribution of selected minor and major components in the painting may be visualized. The use of high-intensity X-ray beams leads to sufficiently small data acquisition dwell times per pixel so that large, decimeter-sized areas can be scanned. Using lower-energy X-ray beams, Bergmann et al.[30,31] used the same method to reveal the original (Fe rich) writing in the Archimedes' palimpsest. Conversely, in oil paintings, to penetrate through an overcoat of lead white of, for example, 50 μm without significant losses, the energy of the fluorescent radiation must be higher than 10 keV.

To demonstrate the suitability of MA-XRF for visualization of hidden paint layers, V. van Gogh's canvas 'Patch of Grass' was examined at HASYLAB.[32] XRR of this painting suggested that below the multicolored landscape, a painted portrait was present (Figure 8). A pencil beam (0.5 mm $\times$ 0.5 mm) of quasi-monochromatic SR with an energy of 38.5 keV was used for scanning an area of approximately 17.5 cm $\times$ 17.5 cm, corresponding to the position of the covered head. A dwell time of 2 s per pixel was employed, making the total scan time approximately 2 days. Next to chemical elements corresponding to the landscape in the upper layer, such as Cr (chromium oxide, green), Fe (prussian blue, ochre), and Zn (zinc white), the element Sb (antimony) was present, due to the use of the pigment Naples yellow [lead antimonate, $Pb(SbO_3)_2 \cdot Pb_3(Sb_3O_4)_2$] in the covered portrait. The Sb map revealed the details of a female portrait (Figure 9); the maxima in the Sb distribution corresponded to the lighter tones of the portrait, while in the Hg map, van Gogh's use of red accents (via the use of the red pigment vermillion, HgS) was reflected. The approximate reconstruction of the portrait based on the Sb and Hg maps presents a significantly clearer and more detailed image of the hidden composition than the XRR and IRR images (Figure 8b,c). Individual brushstrokes and all physiognomic details could be visualized. The reddish intensity of the flesh tones of the lips, cheek, and forehead adds to the readability of the portrait. Several overpainted works by Rembrandt were successfully examined by means of the same method.[33] Because of the requirement to transport paintings to SR facilities and the scarcity of irradiation time represent significant limitations, activities have been started to construct an optimized X-ray tube-based MA-XRF scanner that may be employed in musea.

3. Infrared Radiation-Based Methods

While X-ray-based techniques are very suitable for visualizing the internal distribution of inorganic, high-*Z* (*Z* being the atomic number) components in artworks such as lead white, vermillion, and Naples yellow, they do yield information about the distribution of low-*Z* components in the substructure of paintings. The heavy metal compounds (and especially the omnipresent lead white) tend to obscure or completely absorb the signals of lower-*Z* materials that they cover or are mixed with, yet some of these components (e.g., chalk, graphite, and ochre) are frequently employed for underdrawing or underpainting.

FIGURE 8. 'Patch of Grass' by V. Van Gogh: (a) optical photograph and (b) XRR and (c) IRR images of the area indicated by the red square in panel a. Reprinted with permission from ref 32. Copyright 2008 American Chemical Society.

Over the past several decades, IRR has become a routine form of analysis in many painting collections, almost exclusively for the study of carbon-based underdrawings. Recently, new infrared methods such as OCT and THz-TDS have emerged, adding the possibility of incorporating depth profiling (OCT), as well as material-specific classification (THz-TDS imaging) in the infrared imaging domain.

3.1. Infrared Reflectography. IRR was introduced in the 1960s[34,35] and uses an IR source of ~1200 nm to illuminate objects. The radiation (900−1700 nm) reflected by the object is recorded with a GaAs-array sensor yielding images with a resolution of up to 0.1 mm, covering areas of typically 0.5−0.5 m^2. IRR is most suitable for the study of underdrawings that consist of infrared absorbing carbon black on reflective chalk or gypsum grounds, as found in paintings from the 16th Century and earlier. Note the detailed and sharp rendering of the contour lines delineating the figures in Figure 10. Examination with IRR of 17th or 18th Century paintings tends to be less rewarding because these later paintings often were set up in sketchy touches of earth pigments or underdrawn in white chalk. These pigment are very poor infrared absorbers. Furthermore, many 17th Century paintings were done on non-infrared-reflective colored grounds. Many of the paints contain infrared absorbing pigments, such as carbon black, that make it hard to distinguish the underdrawings from the covering paint layers.

3.2. Optical Coherence Tomography (OCT). A promising new development is OCT,[36,37] a point scanning method based on the use of a near-IR source coupled to a Michelson

FIGURE 9. (a) Result of macro-XRF scanning of the central 15 cm × 15 cm area of 'Patch of Grass', V. Van Gogh, revealing the portrait of a peasant woman inside the read square indicated in Figure 8a. (b and c) Some comparable portraits of peasant women from the same period by V. Van Gogh. Reprinted with permission from ref 32. Copyright 2008 American Chemical Society.

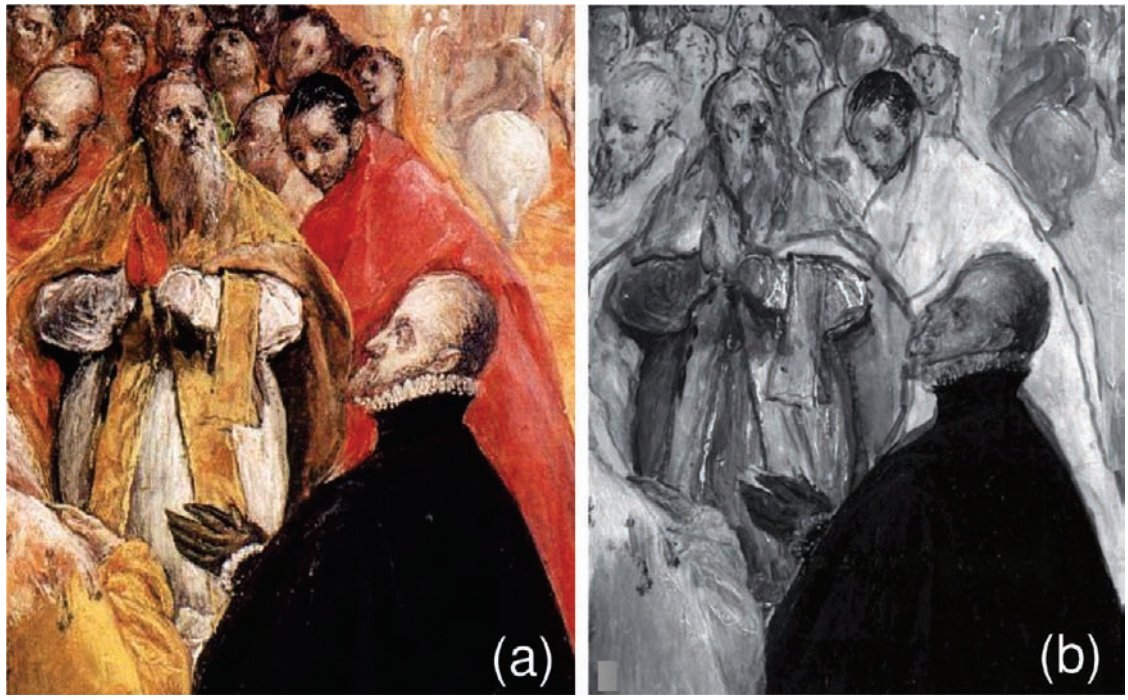

FIGURE 10. Detail of 'Adoration of the Name of Jesus' (1578−1580) by El Greco. (a) Photograph and (b) IRR image showing the contour lines in the underdrawing of the figures adjacent to Philip II (in the black coat).

interferometer. The source, similar to those used for conventional IRR, illuminates both a reference mirror and the object under examination. Constructive interference occurs when the length of the optical path of the light that is backscattered within the object matches, within the coherence length, the length of the optical path of the radiation reflected by the mirror. The interference

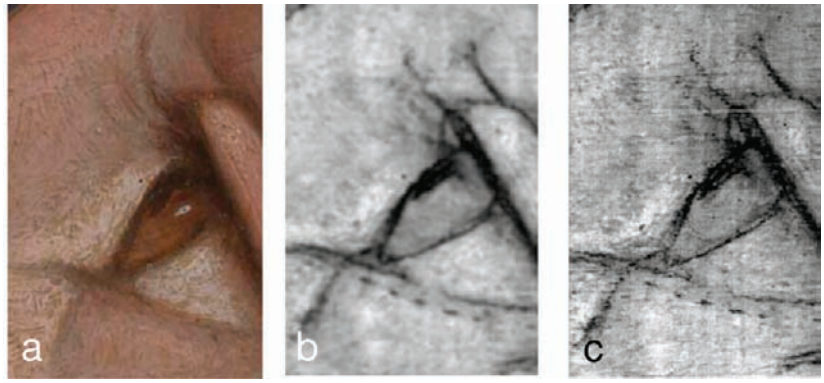

FIGURE 11. (a) Francesco Francia, 'The Virgin and Child with an Angel' (NG 3927), detail of the angel's eye. Copyright The National Gallery, London. (b) Infrared image of the same region using the OSIRIS camera. (c) *En-face* OCT image at 930 nm. The size of the area on the painting is 10 mm × 15 mm.

measurement permits the determination of the depth at which the reflection took place within the object. This adds depth resolution to the infrared investigation of paintings, allowing mapping of the distribution of specific materials and material interfaces throughout the paint stratigraphy. This can be done in the form of cross sections that are perpendicular or parallel (*en-face* OCT) to the paint surface. Series of such maps can be combined to yield three-dimensional information about entire volumes within a painting. The depth resolution of this method is in the single-micrometer range, while the maximum probing depth depends on the thickness of the paint layers and the opacity of the composing materials in the IR domain. Because the technique is based on the collection of single-point measurements, the acquisition is slower than in the case of IRR; in a few hours, it is possible to examine decimeter-sized areas. For the study of thinly painted layers, as found in works from the 16th Century and earlier, the technique proves to be a powerful imaging tool, in particular for the study of near-surface features, notably translucent layers such as glazes and varnish. However, OCT is unable to penetrate thick and opaque paint layers, as mostly present in post-16th Century paintings. Figure 11 compares an *en-face* OCT image to a conventional IRR map. The depth selectivity renders the OCT image more sharp, allowing individual strokes in the underdrawing to be visualized.

3.3. Terahertz Imaging. Far-infrared or terahertz pulses can also be used to detect the presence of hidden paint layers in paintings. The technique works by using an extremely short, focused THz pulse to illuminate a painting, either from the canvas side or from the front side. The back-reflected THz pulse is analyzed for reflections originating from the various interfaces present in the painting, such as the canvas-ground interface and the interfaces between the various paint layers. The temporal spacing between the reflections is a measure of the optical thickness of the paint layers, whereas their sign and amplitude provide information about the THz refractive index contrast between the different layers.

In this sense, the method works in a manner similar to that of "acoustic echo" equipment (medical imaging). THz spectroscopy is a noncontact technique: THz pulses are focused on the painting from a distance of ~10 cm. T-rays do not ionize the material, and the extremely low intensities employed rule out adverse effects on the painting. Moreover, the refractive-index contrast in the THz range is larger than in the visible and near-infrared (VIS/NIR) region, making it easier to observe contrast between the paint layers even if they are very thin (<20 μm). The greatest advantage is the ability of T-rays to fully penetrate the painting, allowing observation of reflections from the various interfaces at all depths below the surface. This is not possible with VIS or NIR radiation. Figure 12 shows preliminary results from a test panel consisting of strokes of a number of different thickness covered by a layer of lead white. Next to revealing the position of the individual strokes, the variation in the thickness of the umber layer is apparent.[38]

4. Conclusions and Perspectives

Since 2005, several new variants of IRR and XRR, the traditional methods employed by the art and museum world to inspect and examine the inner, multilayered structure of paintings, have been developed. Currently, the first reports on realistic case studies are appearing in the literature. Some of the new variants feature depth selectivity, while others offer element- or pigment-specific imaging information.

By means of a combination of energetic X-rays, appropriate detectors, and optics, either depth-selective or projected elemental distributions in the subsurface region of paintings may be obtained; since, in any case, the fluorescent signals must escape through strongly absorbing layers of paint, the

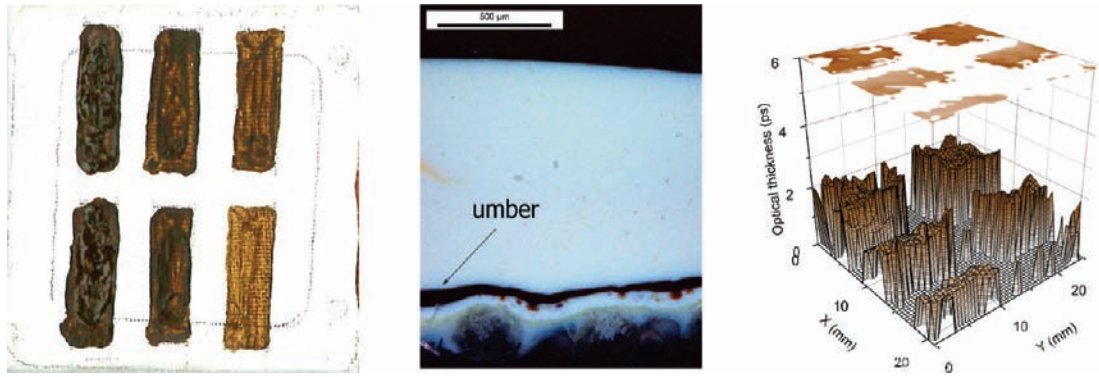

FIGURE 12. Test panel with strokes of umber, subsequently covered with a layer of lead white (left). Cross-section THz map of the umber/lead white interface (middle) reveals the variation in paint layer thickness in the stratigraphy of the lower left stroke (right).

information obtained in this manner is usually, but not in all cases, limited to the top 100−200 μm below the surface and to elements with fairly energetic (>8 keV) characteristic lines, i.e., $Z \geq 29$ (Cu).

On the other hand, by means of the recently developed variants of IRR, low-Z materials such as charcoal, chalk, and ochre that are often used for underpainting or underdrawing can be visualized in greater detail and with greater depth selectivity.

Thus, it becomes possible to employ the different state-of-the-art variants of XRR and IRR in a complementary fashion to obtain a more complete picture of a painting and many of its superimposed paint layers.

This research was supported by the Interuniversity Attraction Poles Programme-Belgian Science Policy (IUAP VI/16). The text also presents results of FWO (Brussels, Belgium) projects nr. G.0704.08 and G.0179.09 and from the UA-BOF GOA programme.

BIOGRAPHICAL INFORMATION

Koen Janssens obtained his Ph.D. in Analytical Chemistry from the University of Antwerp and became a professor at this university in 2000. He has employed since 1990 intense beams of X-rays for nondestructive materials analysis. His main field of interest is X-ray-based microanalysis of materials, with special attention paid to local speciation of metals in (altered) environmental and cultural heritage materials such as glass and inorganic painters' pigments.

Joris Dik trained as art historian at the University of Amsterdam and then obtained a Ph.D. in X-ray crystallography at the Free University of Amsterdam (Amsterdam, The Netherlands), focussing on the synthesis and alteration behavior of the pigment lead-tin yellow. His research interest is the application of novel methods of scientific investigation to art historical problems. He currently is an associate professor at the Delft University of Technology.

After gaining the "agrégation" of chemistry at the "Ecole Normale Supérieure" of Lyon, **Marine Cotte** obtained a Ph.D. in lead-based cosmetics and pharmaceutical compounds used in Antiquity at C2RMF (Centre of Research and Restoration of French Museums, Paris, France). During her postdoc at the European Synchrotron Radiation Facility (ESRF), she has broadened the application of micro X-ray and FTIR spectroscopies to paintings. She currently has a twofold position as a permanent CNRS scientist at C2RMF and as a beamline scientist at ESRF.

Jean Susini obtained his Ph.D. in Chemical Physics at the University Pierre et Marie Curie (Paris, France) and joined the ESRF in 1989, where he became responsible for the research and development of X-ray mirrors for synchrotron beamlines. In 1994, he took responsibility for the design, construction, and operation of the X-ray microscopy beamline. In 2009, he was appointed Head of the Instrumentation Services and Development Division of ESRF. He is also a regular lecturer at the University Joseph Fourier (Grenoble, France) and at the University Pierre et Marie Curie. His main fields of interest are X-ray optics, X-ray imaging techniques, and their applications.

REFERENCES

1 van de Wetering, E. *The Painter at Work*; Amsterdam University Press: Amsterdam, 2000.

2 Hendriks, E. Van Gogh's working Practice: A technical study. In *New Views on Van Gogh's Development in Antwerp and Paris: An integrated Art Historical and Technical study of his Paintings in the Van Gogh Museum*; Hendriks, E., Van Tilborgh, L., Eds.; University of Amsterdam: Amsterdam, 2006; pp 231−245.

3 Khandekar, N. Preparation of cross sections from easel paintings. *Rev. Conserv.* **2003**, *4*, 52–64.

4 Van Heugten, S. Radiographic images of Vincent van Gogh's painting in the Kröller-Müller Museum, Otterlo, and the Van Gogh Museum, Amsterdam. In *Van Gogh Museum Journal*; Van Gogh Museum: Amsterdam, 1995; pp 63−85.

5 van Kaick, G.; Delorme, S. Computed tomography in various fields outside medicine. *Eur. Radiol.* **2005**, *15*, D74–D81.

6 Huppertz, A.; Wildung, D.; Kemp, B. J.; Nentwig, T.; Asbach, P.; Rasche, F. M.; Hamm, B. Nondestructive Insights into Composition of the Sculpture of Egyptian Queen Nefertiti with CT. *Radiology* **2009**, *251*, 233–240.

7 Janssen, R.; Poulus, M.; Kottman, J.; De Groot, T.; Huisman, D. J.; Stoker, J. CT: A new nondestructive method for vizualising and characterizing Ancient Roman glass fragments in situ in blocks of soil. *Radiographics* **2006**, *26*, 1837–1844.

8 Bugani, S.; Camaiti, M.; Morselli, L.; Van de Casteele, E.; Janssens, K. Investigating morphological changes in treated vs. untreated stone and building materials by X-ray micro-CT. *Anal. Bioanal. Chem.* **2008**, *391*, 1343–1350.

9 Bugani, S.; Modugno, F.; Lucejko, J. J.; Giachi, G.; Cagno, S.; Cloetens, P.; Janssens, K.; Morselli, L. Study on the impregnation of archaeological waterlogged wood with consolidation treatments using synchrotron radiation microtomography. *Anal. Bioanal. Chem.* **2009**, *395*, 1977–1985.

10 Attwood, D. Microscopy: Nanotomography comes of age. *Nature* **2006**, *442*, 642–643.

11 Reischig, P.; Blaas, J.; Botha, C.; Bravin, A.; Porra, L.; Nemoz, C.; Wallert, A.; Dik, J. A note on medieval microfabrication: The visualization of a prayer nut by synchrotron-based computer X-ray tomography. *J. Synchrotron Radiat.* **2009**, *16*, 310–313.

12 De Nolf, W.; Janssens, K. Micro X-ray diffraction and fluorescence tomography for the study of multilayered automotive paints. *Surf. Interface Anal.* **2010**, *42*, 411–418.

13 Weitkamp, T.; David, Ch.; Bunk, O.; Bruder, J.; Cloetens, P.; Pfeiffer, F. X-ray phase radiography and tomography of soft tissue using grating interferometry. *Eur. J. Radiol.* **2008**, *68S*, S13—S17.

14 Tafforeau, P.; Smith, T. A. Nondestructive imaging of hominoid dental microstructure using phase contrast X-ray synchrotron microtomography. *J. Hum. Evol.* **2008**, *54*, 272–278.

15 Lak, M.; Fleck, G.; Azar, D.; Engel, M.; Kaddumi, H.; Neraudeau, D.; Tafforeau, P.; Nel, A. Phase contrast X-ray synchrotron microtomography and the oldest damselflies in amber (Odonata: Zygoptera: Hemiphlebiidae). *Zool. J. Linnean Soc.* **2009**, *156*, 913–923.

16 Boon, J. J.; Ferreira, E. S. B.; Van Der Horst, J.; Stampanoni, M.; Marone, F. X-ray tomographic microscopy compared to ion polished paint cross sections of 19th century paints with and without metal soap aggregates. In *Book of Abstracts*;TECHNART 2009 Conference, April 2009, Athens; p 39.

17 Keune, K.; Boon, J. J. Analytical imaging studies of cross-sections of paintings affected by lead soap aggregate formation. *Stud. Conserv.* **2007**, *52*, 161–176.

18 Helfen, L.; Baumbach, T.; Cloetens, P.; Baruchel, J. Phase-contrast and holographic computed laminography. *Appl. Phys. Lett.* **2009**, *94*, 104103.

19 Krug, K.; Porra, L.; Coan, P.; Wallert, A.; Dik, J.; Coerdt, A.; Bravin, A.; Reischig, P.; Elyyan, M.; Helfen, L.; Baumbach, T. Relics in Medieval Altarpieces? Combining X-ray Tomographic, Laminographic and Phase-Contrast Imaging to Visualize Thin Organic Objects in Paintings. *J. Synchrotron Radiat.* **2008**, *15*, 55–61.

20 Dik, J.; Reischig, P.; Krug, K.; Wallert, A.; Coedrt, A.; Helfen, L.; Baumbach, T. Three-dimensional Imaging of Paint Layers and Paint Substructures with Synchrotron Radiation Computed α-Laminography. *J. Am. Inst. Conserv.* **2009**, *28*, 185–197.

21 Bertrand, L.; Vantelon, B.; Pantos, E. Novel interface for cultural heritage at SOLEIL. *Appl. Phys. A: Mater. Sci. Process.* **2006**, *83*, 225–228 (see also http://www.synchrotron-soleil.fr/heritage).

22 Cotte, M.; Susini, J.; Dik, J.; Janssens, K. Synchrotron-Based X-ray Absorption Spectroscopy for Art Conservation: Looking Back and Looking Forward. *Acc. Chem. Res.* **2010**, *43*, 000 (in press).

23 Van der Snickt, G.; Dik, J.; Cotte, M.; Janssens, K.; Jaroszewicz, J.; De Nolf, W.; Groenewegen, J.; Van der Loeff, L. Characterization of a Degraded Cadmium Yellow (CdS) Pigment in an Oil Painting by Means of Synchrotron Radiation Based X-ray Techniques. *Anal. Chem.* **2009**, *81*, 2600–2610.

24 Derrick, M.; Souza, L.; Kieslich, T.; Florsheim, H.; Stulik, D. Embedding paint cross-section samples in polyester resins: Problems and solutions. *J. Am. Inst. Conserv.* **1994**, *33*, 227–245.

25 Kanngiesser, B.; Mantouvalou, I.; Malzer, W. Non-destructive, depth resolved investigation of corrosion layers of historical glass objects by 3D Micro X-ray fluorescence analysis. *J. Anal. At. Spectrom.* **2008**, *23*, 14-819.

26 Janssens, K.; Proost, K.; Falkenberg, G. Confocal microscopic X-ray fluorescence at the HASYLAB microfocus beamline: Characteristics and possibilities. *Spectrochim. Acta, Part B* **2004**, *59*, 1637–1642.

27 Kanngiesser, B.; Malzer, W.; Reiche, I. A new 3D micro X-ray fluorescence analysis set-up: First archaeometric applications. *Nucl. Instrum. Methods Phys. Res., Sect. B* **2003**, *211*, 259–264.

28 Kanngiesser, B.; Malzer, W.; Rodriguez, A. F.; Reiche, I. Three-dimensional micro-XRF investigations of paint layers with a tabletop setup. *Spectrochim. Acta, Part B* **2005**, *60*, 41–47.

29 Woll, A. R.; Mass, J.; Bisulca, C.; Cushi-Nan, M.; Griggs, C.; Wanzy, T.; Ocon, N. The Unique History of The Armorer's Shop, An Application of Confocal X-ray fluorescence microscopy. *Stud. Conserv.* **2008**, *53*, 93–109.

30 Bergmann, U. Archimedes brought to light. *Phys. World* **2007**, *20*, 39–42.

31 Service, R. F. Imaging: Brilliant X-rays reveal fruits of a brilliant mind. *Science* **2006**, *313*, 744–745.

32 Dik, J.; Janssens, K.; van der Snickt, G.; van der Loeff, L.; Rickers, K.; Cotte, M. Visualization of a Lost Painting by Vincent van Gogh Using Synchrotron Radiation Based X-ray Fluorescence Elemental Mapping. *Anal. Chem.* **2008**, *80*, 6436–6442.

33 van de Wetering, E. Rembrandt Laughing c. 1628: A painting resurfaces. In *Kroniek van het Rembrandthuis*; Rembrandthuis: Amsterdam, 2007; pp 18—40.

34 Van Asperen de Boer, J. R. J. An introduction to the scientific examination of paintings. In *Scientific examination of early Netherlandish painting*; Filedt-Kok, J. P., Van Asperen-De Boer, J. R. J., Eds.; Fibula-van Dishoeck: Bussum, The Netherlands, 1976; pp 1—40.

35 Saunders, D.; Billinge, R.; Cupitt, J.; Atkinson, N.; Liang, H. A new camera for high-resolution infrared imaging of works of art. *Stud. Conserv.* **2006**, *51*, 277–290.

36 Liang, H.; Cid, M. G.; Cucu, R. G.; Dobre, G. M.; Podoleanu, A. Gh.; Pedro, J.; Saunders, D. En-face Optical Coherence Tomography: A novel application of noninvasive imaging to art conservation. *Opt. Express* **2005**, *13*, 6133–6144.

37 Hughes, M.; Spring, M.; Podoleanu, A. Speckle noise reduction in optical coherence tomography of paint layers. *Appl. Opt.* **2010**, *49*, 99–107.

38 Adam, A. J. L.; Planken, P. C. M.; Meloni, S.; Dik, J. TeraHertz imaging of hidden paint layers on canvas. *Opt. Express* **2009**, *17*, 3407–3416.